CHEMICAL ENGINEERING TRANSACTIONS
VOL. 94, 2022
A publication of AIDIC
The Italian Association of Chemical Engineering
Online at www.cetjournal.it
Guest Editors: Petar S. Varbanov, Yee Van Fan, Jiří J. Klemeš, Sandro Nižetić

ISBN 978-88-95608-93-8; **ISSN** 2283-9216
DOI: 10.3303/CET2294101

Investigation of Drop Size in Liquid-Liquid Dispersion Agitated by Sawtooth Impeller: Effect of Optical Measuring Device

Roman Formánek*, Radek Šulc

Czech Technical University in Prague, Faculty of Mechanical Engineering, Department of Process Engineering, Technická 4, 160 00 Prague, Czech Republic
Roman.Formanek@fs.cvut.cz

Experimental measurement of drop size in immiscible liquid-liquid dispersion using non-disruptive in-situ non-invasive method utilizing high-speed image capturing and Image Analysis strongly depends on the quality of captured images. This contribution aims to analyze the effect of optical properties of the image acquisition system on the determination of the drop size in a baffled vessel agitated by a high-shear sawtooth impeller. The experiments were carried out for three impeller speeds at low dispersed phase volume fraction when the drop breakage occurs only.

1. Introduction

The drop size distribution is a crucial property in particulate processes and which is affected by many quantities and factors - a flow of suspensions, dispersions, possible separation processes, mass transfer, vessel configuration, impeller type, etc. Experimental measurement of drop size in immiscible liquid dispersion systems has still been challenging and the measurements methods used can be divided into two groups: i) ex-situ measurement methods and ii) in-situ measurement methods. The ex-situ measurement method is based on the withdrawal of the dispersion sample from the dispersed system. The in-situ measurement method can be further subdivided into invasive measurement and non-invasive measurement. The invasive measurement method used an optical probe placed directly in a mixed volume. Endoscope measurement technique (Kraume et al., 2004) or video probe (Khalil et al., 2010) were often used. The immersed probe affects the velocity field, which is a disadvantage of this method. Non-invasive measurement method usually uses high-speed image capture of the investigated area to determine the drop size (Maaß and Kraume, 2012) or the interferometric particle imaging and shadowgraph method (Jasikova et al., 2018). The quality of the captured images is crucial to obtain credible drop sizes. Beside main known parameters such as shutter speed, frame rate, and focus depth, the quality of captured images depends also significantly on the raw image background, which is mainly affected by the type of the light source (Bucciarelli et al., 2019). Formanek et al. (2019a) tested the effect of four types of light sources on image quality. They carried out the following tests to determine: i) the effect of light source position on a background colour, ii) the effect of shutter speed on a background colour, and iii) the effect of shutter speed on the accuracy of evaluated particle size. They found that the halogen lamp and the commercial light-emitting diode (LED) panel generate a grey image background, resulting in a low number of identified particles. Unlike this, the designed light sources 60 W LED chip and 90 W LED chip ensure a practically white image background that is insensitive to the installed source position. This contribution aims to analyze the effect of optical properties of the image acquisition system on drop size determination in immiscible liquid-liquid dispersion using an in-situ non-invasive method utilizing high-speed image capturing and Image Analysis (IA). Two objectives of different optical properties were used for comparison. The experiments were carried out in a baffled vessel agitated by a high-shear sawtooth impeller for three impeller speeds at a low dispersed phase volume fraction when the drop breakage occurs only. As an immiscible liquid-liquid system, a mixture of distilled

Paper Received: 15 May 2022; Revised: 13 June 2022; Accepted: 20 June 2022
Please cite this article as: Formánek R., Šulc R., 2022, Investigation of Drop Size in Liquid-Liquid Dispersion Agitated by Sawtooth Impeller: Effect of Optical Measuring Device, Chemical Engineering Transactions, 94, 607-612 DOI:10.3303/CET2294101

water and silicone oil was used. Two criteria were used for the evaluation of image acquisition quality: i) the number of evaluated drops and ii) the drop size distribution (DSD).

2. Methods

2.1 Experimental set-up

The experiments were carried out in an agitated vessel with standard cylindrical geometry with flat bottom and with four radial baffles (see Figure 1). The image acquisition system consists of: i) a single-point light source with a 90 W LED chip, and ii) a high-speed camera SpeedSence MK III equipped with the optical objective. The two different objectives were tested: i) Sigma 105 mm F2.8 EX DG MACRO objective being the objective with longer foccus length and higher sharpness depth, and ii) Laowa 60 mm f 28 Ultra-Macro 2:1 objective being the objective with shorter focal length and lower sharpness depth. The image capture was provided by a high-speed camera with a frame rate lowered to 30 fps, a shutter time of 0.1 ms, and a full resolution of 1,280 x 1,024 pixels. The frames were captured in the region under the impeller (see Figure 1). The parameters of the captured region and images of both objectives are given in Table 1. The experiments were carried out at three different impeller rotational speeds, 750, 850, and 950 rpm (Reynolds number 127,296; 144,268; and 161,241 respectively). The average temperature of the immiscible liquid-liquid system was 21.1 °C during the experiment. The model liquid was distilled water and WACKER AP 200 (density = 1,076.7 kg/m^3, dynamic viscosity = 232 mPa). The used of the dispersed oil phase volume fraction was 0.0047. The oil was added prior to measurements by syringe injection.

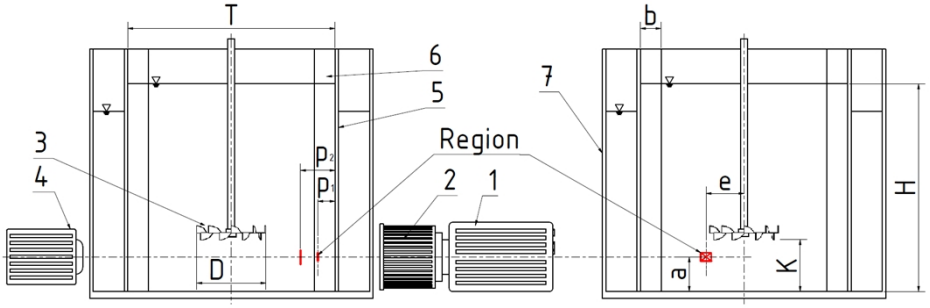

Figure 1: Scheme and arrangement of the experimental device 1, High-speed camera (SpeedSence MKIII – Dantec Dynamics, Denmark) 2, Macro objective 3, Sawtooth impeller 4, Single-point light source 5, Cylindrical vessel wall 6, Baffles 7, Optical box, Vessel inner diameter T = 300 mm, Impeller diameter D = T/3, Baffle width b = 0.1T, Liquid level H = T, Impeller off-bottom distance K = T/4, Region off-bottom distance a = 50 mm, Distance of regions from vessel wall for Laowa objective p_1 = 25 mm, Distance of regions from vessel wall for Sigma objective p_2 = 50 mm, Region distance from the shaft e = 55 mm

Table 1: The parameters of captured region and images

Objective	Area of Region [mm]	Image resolution [mm/pixel]	Sharpness depth* [mm]	Measurement error** [%]
Sigma	approx. 15 x 12	0.01176	1.75	0.038
Laowa	approx. 7.5 x 6.5	0.00605	1.24	0.034

*Sharpness depth was evaluated experimentally by the preparation.

** n measurement error was included the influence of image resolution determination, sharpness depth, and influence of increasing temperature through the experiment.

2.2 Data analysis

The following procedure given by Formánek and Šulc (2020) was adopted: i) 1,000 images were captured during each recording set (the total recording time was 33.3 s), ii) the first set of images was taken 5 minutes after the impeller speed was changed, iii) the recording was repeated after 5 minutes until the time of 50 minutes was reached, the impeller speed was increased, and the procedure was repeated. The calibration procedure was used to determine image resolution using the 1 x 1 mm grid (see Figures 2a and 2b) and the precise diameter for the determination of the image analysis parameters for both optical objectives. The approach based on the sharp boundary used by Formánek et al. (2019b) was adopted for size determination. The sharp boundary was estimated using the pixel shade gradient. This method compares neighbouring pixels and evaluates the gradient

between them and equates to a set gradient value. Setting a high gradient value, unfocused objects with blurred borders can be eliminated and objects with sharp borders can be evaluated only. The drops were identified from captured images, and their equivalent drop diameter calculated according to the projected area was determined for a given stirring time and impeller speeds. For illustration, the raw images captured by both optical objectives at a recording time of 5 minutes at the impeller speed of 850 rpm are presented in Figures 2c and 2d.

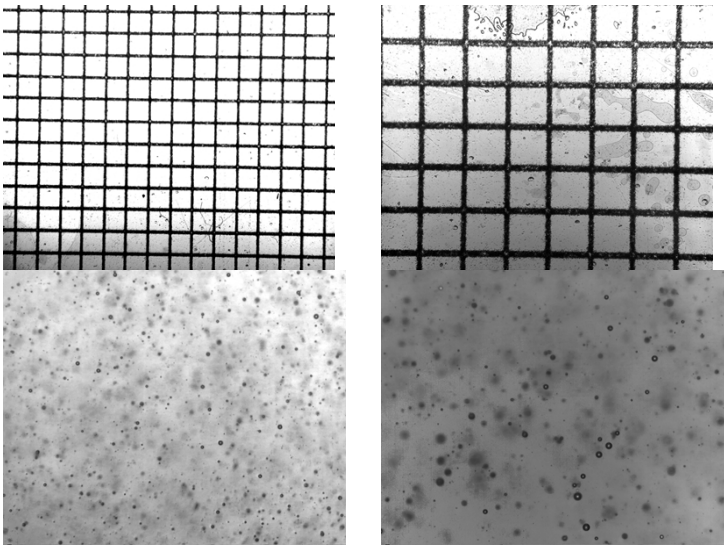

Figure 2: Captured images: a) 1 x 1 mm grid captured by Sigma objective (upper left); b) 1 x 1 mm grid captured by Laowa objective (upper right); c) Raw image captured by Sigma objective at recording time of 5 min at the impeller speed of 850 rpm (bottom left), d) Raw image captured by Laowa objective at recording time of 5 min at the impeller speed of 850 rpm (bottom right)

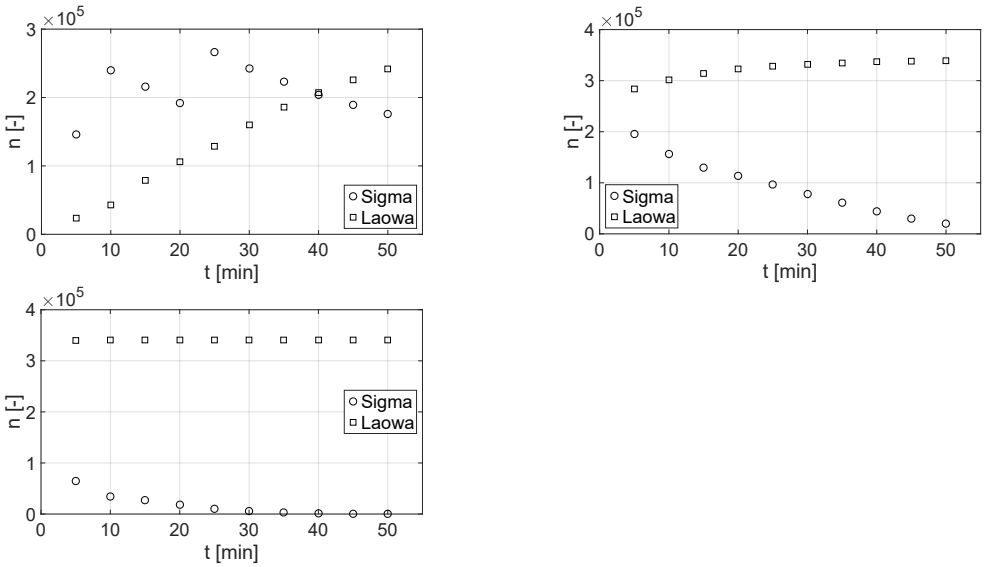

Figure 3: The time courses of the number of evaluated drops: a) 750 rpm impeller speed (upper left); b) 850 rpm impeller speed (upper right); c) 950 rpm impeller speed (bottom left)

3. Results and Discussion

3.1 Number of evaluated drops

Bucciarelli et al. (2019) reported that the minimum number of evaluated drops must be reached to obtain relevant results. Therefore, the number of drops evaluated was used as the first evaluation criterion. The time courses

of the number of evaluated drops are shown in Figure 3 for both the objectives tested and three impeller rotation speeds. The total number of evaluated drops represents the sum of identified drops from 30,000 captured images (10 sets by 1,000 images for each impeller speed). Due to drop breaking, the drop size decreases and the number of formed drops decreases over time.
Using the objective with a longer focus length and higher sharpness depth (Sigma objective), the number of evaluated drops was on average around 200,000 in each recording set for 750 rpm impeller speed. Some jumps in the number of evaluated drops were observed in measuring time from 5 to 10 minutes and from 20 to 25 minutes. For the impeller speed at 850 rpm, the number of evaluated drops continually decreased from 200,000 per recording set to 19,900 per set at the end of the measurement. For the highest impeller speed, 950 rpm, the number of drops evaluated from images obtained using this objective was many times lower. For a measurement time longer than 30 min, the number of evaluated drops was less than 6,200.
The objective with a shorter focal length and lower sharpness depth (Laowa objective) exhibited the highest performance for higher impeller speeds, 850 and 950 rpm. The number of drops evaluated was on average greater than 300,000 in each set of records. Unlike this, the performance for the 750 rpm impeller speed was lower compared to the Sigma objective. The number of evaluated drops continued to increase from 23,500 per recording set to 241,000 per set at the end of the measurement.

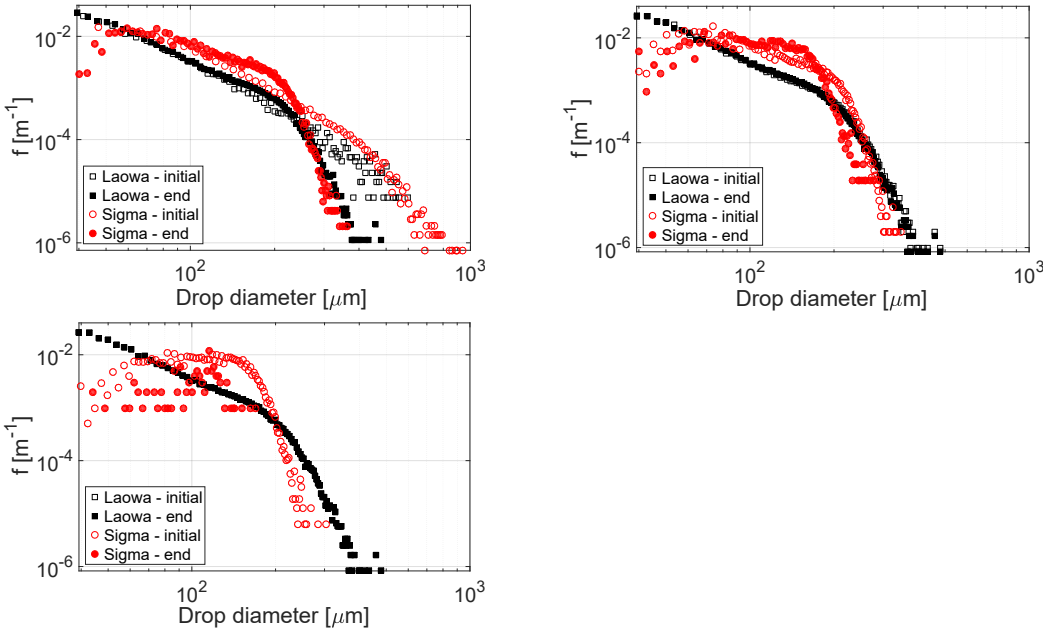

Figure 4: Frequency drop size distribution at the beginning (initial = 5 min) and at the end of the measurement (end = 50 min) for both investigated objectives: a) 750 rpm impeller speed (upper left); b) 850 rpm impeller speed (upper right); c) 950 rpm impeller speed (bottom left)

3.2 Frequency drop size distribution

The frequency drop size distribution was used as the second criterion for comparison. The frequency drop size distribution plotted on the logarithm scale is presented in Figure 4 for both the tested objectives and three impeller rotation speeds. The distribution curves obtained at the beginning (initial = 5 min) and at the end of the measurement (end = 50 min) are rendered. The differences between objectives are significant and visible.
The objective with a longer focal length and lower sharpness depth (Laowa objective) exhibited more consistent DSD behaviour for all three impeller speeds compared to the objective with a lower focus length and higher sharpness depth (Sigma objective). DSD exhibits two different regions with boundary drop sizes around 110 μm. For lower drop sizes, the DSD practically does not change over time. The breakage of drops greater than 110 μm is visible for the 750 rpm impeller speed. For higher impeller speeds used, the changes are smaller, and for 950 rpm practically negligible.
The distribution obtained using the objective with longer focus length and higher sharpness depth (Sigma objective) is roughly comparable with the previous, only for 750 rpm impeller speed. The initial frequency of the drops captured by the Sigma objective is slightly less than the frequency of drops captured by the Laowa

objective. At the end of the measurement (50 min), the frequency of drops captured by the Sigma objective in the size range from 70 to 125 μm is higher than the frequency of drops captured by the Laowa objective. The DSD obtained by the Laowa objective also exhibits a lower number of smallest drops. The frequency of smallest drops captured by the Sigma objective is an order of magnitude smaller than for the Sigma objective. The discrepancies between DSDs increase with higher impeller speeds tested. For the highest impeller speed of 950 rpm, the DSD determined at the end of measurement is incredible, probably due to the low number of captured drops.

3.3 Effect of mixing intensity

The kinetic model determined by Hong and Lee (1983) was used for the evaluation of equilibrium Sauter mean diameter d_{32}^* for each impeller speed and both objectives. Assuming the Kolmogorov theory of turbulence (Kolmogorov, 1941), the Kolmogorov length scale for the closest area of the impeller was estimated to be 11 μm in size. The minimal drop size evaluated was around 29 μm; and the breakup occurs in the inertial subrange and the drop breakup is controlled by inertial forces. In this case and assuming that $\varepsilon \propto N^3D^2$, the dimensionless equilibrium Sauter mean diameter defined as the ratio d_{32}^*/D depends on the impeller Weber number We as follows (Hinze, 1955):

$$\frac{d_{32}^*}{D} = C_1\, We^{-0.6} \tag{1}$$

where C_1 is the constant of proportionality depending on system geometry, D [m] is the impeller diameter, and We [-] is the impeller Weber number. The comparison of the experimental values and the expected dependence given by Eq(1) is presented in Figure 5.

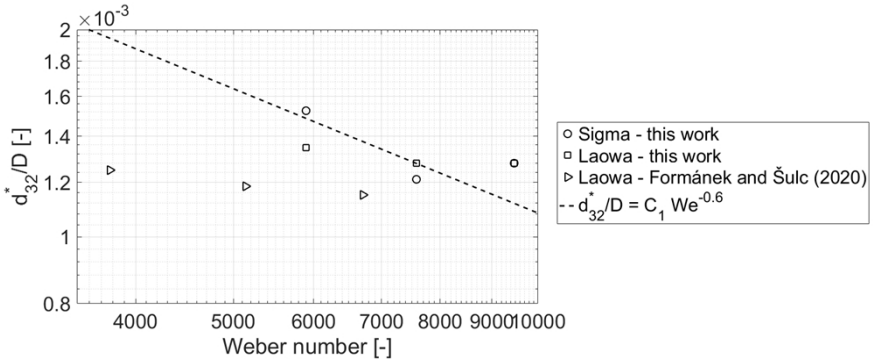

Figure 5: Effect of mixing intensity – dependence of dimensionless equilibrium Sauter mean diameter on impeller Weber number

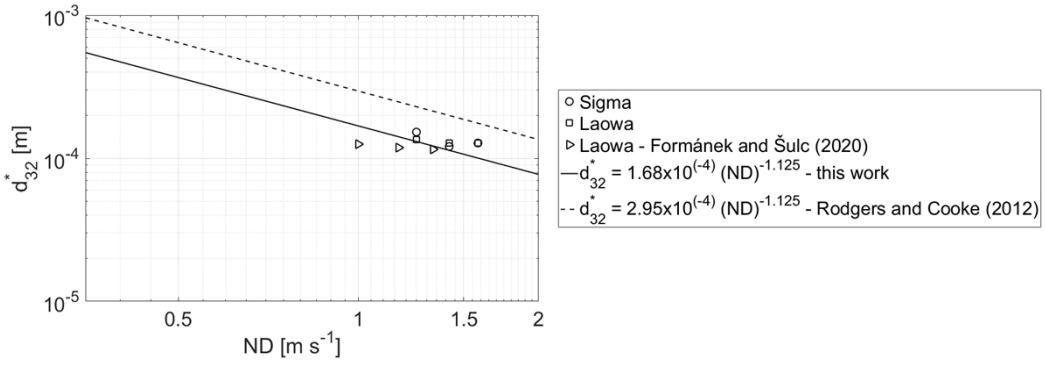

Figure 6: Effect of mixing intensity – dependence of equilibrium Sauter mean diameter on shear tip speed

The value of equilibrium Sauter mean diameter determined using the Sigma objective was approximately 20 μm higher than the value determined by the Laowa objective at the impeller speed of 750 rpm (We = 5,900). For the impeller speed of 850 rpm (We = 7,578), the d_{32}^* diameter determined using the Sigma objective was approximately 10 μm lower than the value determined using the Laowa objective. For the impeller speed of 950

rpm (We = 9,466), the values of the equilibrium Sauter mean diameters were similar for both objectives used. By regression, the value of the proportionality constant C_1 = 0.27 was obtained. For comparison, the data obtained for lower impeller speeds using the Laowa objective are presented (Formánek and Šulc, 2020). In this case, the proportionality constant of 0.195 was determined for the same geometrical system.
Unlike this, Rodgers and Cooke (2012) proposed the shear tip speed as a correlating parameter for the dependence of d_{32}* diameter on mixing intensity as follows:

$$d_{32}^{*} \sim C_2\,(ND)^{-1.125} \tag{2}$$

The comparison of experimental data and the prediction given by Eq(2) is shown in Figure 6. The shear tip speed seems to be more suitable as a correlating parameter characterizing the effect of mixing intensity on drop size for the tested system and conditions.

4. Conclusions

The in-situ measurement technique followed by the image analysis method was used for the determination of drop sizes and their distribution in a dilute immiscible liquid-liquid dispersion agitated by a high-shear sawtooth impeller. The effect of optical properties of the image acquisition system on the determination of the drop size was investigated. Two objectives of different optical properties were used for comparison. Two criteria were used for the evaluation of image acquisition quality: i) the number of evaluated drops and ii) the drop size distribution. The objective with a shorter focal length and lower sharpness depth was found to be more suitable for image capture in the tested system with higher impeller speed and small droplet size produced. The findings confirmed that the setting of the acquisition system is crucial to obtain credible results. The shear tip speed proposed by Rodgers and Cooke (2012) as a correlating parameter characterizing the effect of mixing intensity on drop size seems to be more suitable for the system and conditions. The correlation using the impeller Weber number traditionally used was not as convincing for given conditions.

Acknowledgments

This work was supported by GA CTU SGS project number SGS20/119/OHK2/2T/12 “Transport phenomena in multiphase systems” and by the Ministry of Education, Youth and Sports of the Czech Republic under OP RDE grant number CZ.02.1.01/0.0/0.0/16_019/0000753 “Research center for low-carbon energy technologies”.

References

Bucciarelli E., Formánek R., Kysela B., Fořt I., Šulc R., 2019, Dispersion Kinetics in Mechanically Agitated vessel, EPJ Web Conf., 213, 02008.
Formánek R., Kysela B., Šulc R., 2019a, Image analysis of particle size: Effect of Light Source Type, EPJ Web Conf., 213, 02021.
Formánek R., Kysela B., Šulc R., 2019b. Drop Size Evolution Kinetics in a Liquid-Liquid Dispersions System in a Vessel Agitated by a Rushton Turbine, Chem. Eng. Trans., 74, 1039–1044.
Formánek R., Šulc R., 2020, The Liquid–Liquid Dispersion Homogeneity in a Vessel Agitated by a High-Shear Sawtooth Impeller, Processes, 8, 1012.
Hinze J.O., 1955, Fundamentals of the Hydrodynamic Mechanism of Splitting in Dispersion Processes, AIChE J., 1, 289-295.
Hong P.O., Lee J.M., 1983, Unsteady-state Liquid-Liquid Dispersions in Agitated Vessels, Ind. Eng. Chem. Process. Des. Dev., 22, 130–13.
Jasikova D., Kotek M., Kysela B., Sulc R., Kopecky V., 2018, Compiled Visualization with IPI Method for Analysing of Liquid-liquid Mixing Process, EPJ Web Conf., 180, 02039.
Khalil A., Puel F., Chevalier Y., Galvan J.-M., Rivoire A., Klein J.-P., 2010, Study of Droplet Size Distribution during an Emulsification Process using In situ Video Probe Coupled with an Automatic Image Analysis, Chem. Eng. J., 165, 946–957.
Kolmogorov A.N., 1941, The Local Structure of Turbulence in Incompressible Viscous Fluid for Very Large Reynolds' numbers, Doklady Akad. Nauk SSSR, 30, 301.
Kraume M., Gabler A., Schulze K., 2004, Influence of Physical Properties on Drop Size Distribution of Stirred Liquid-Liquid Dispersions, Chem. Eng. Technol., 27, 330–334.
Maaß S., Kraume M., 2012, Determination of Breakage Rates using Single Drop Experiments, Chem. Eng. Sci., 70, 146–164.
Rodgers T.L., Cooke M., 2012, Correlation of Drop Size with Shear Tip Speed, In: Proceedings of the 14th European Conference on Mixing, Warszawa, Poland, B17.